ISSN 1598-2602
Vol. 4-B, No. 1
March 2004

KIEE INTERNATIONAL TRANSACTIONS ON

ELECTRICAL MACHINERY and ENERGY CONVERSION SYSTEMS

THE KOREAN INSTITUTE OF ELECTRICAL ENGINEERS

Characteristic Analysis and Design of Switched Reluctance Motor for the Improved 2-phase Snail-cam Type Fan Motor

Ji-Young Lee*, Geun-Ho Lee* and Jung-Pyo Hong*

Abstract - This paper deals with the design and analysis of a 2-phase Switched Reluctance Motor (SRM) used for the cooling fan motor of a refrigerator. To reduce the dead zone and improve the efficiency, the snail-cam type rotor pole and the asymmetric stator pole are investigated. For the optimal shape design, the performances of each model are obtained from numerical calculation results by 2D time-stepping finite element method (FEM) coupled with circuit equations. The accuracy of analysis is verified by comparing the analysis results with experimental data. According to the investigation results, improved shapes of stator and rotor poles are proposed.

Keywords: Asymmetric stator pole, Finite element method, Snail-cam type, Switched Reluctance Motor

1. Introduction

Switched Reluctance (SR) motors have many advantages, such as possibility of high-speed operation and simplicity of mechanical construction. These characteristics make SR motors a good alternative to other types, such as Brushless DC and induction motors, and a better choice for household electric appliances. In particular, 2-phase SR motors have gained the continuous attention of many researchers due to their low cost [1, 2]. Even though 2-phase SR motors have some attractive qualities, they still have inherited disadvantages such as torque ripple and low efficiency in commercial applications. Therefore, in this paper the design of a 2-phase SR motor is investigated to improve the torque characteristic and efficiency for the fan motor in refrigerators.

For the design of 2-phase SR motors as a component of electric appliances, there are several constraints to be dealt with. The number of stator and rotor poles, number of turns, and outer volume are fixed because the fan load, rated speed, and input voltage are constant and the system is compact. The shape of rotor and stator poles is the only aspect that can be changed. Therefore, four design variables have been selected, the stator pole arc, the ratio of the stator pole arc, the existence of the dip, and rotor slot depth. Analysis models have been made by the combination of these variables, and for each analysis model the average torque and efficiency has been calculated by using a hybrid method combining the 2D finite element method (FEM) with the voltage equation.

2D solvers can be used effectively to estimate the magnetic characteristics of general lamination geometry; however they cannot be expected to provide accurate magnetization curves for SR motors with short axial length because of the significant influence of end effects [1]. Furthermore, the drive characteristic should also be considered since the switching states depending on drive are a great influence on phase current shapes. Therefore, the end effect is considered when inductance is calculated, and the dynamic simulation is accomplished with the consideration of the performance of drives. Finally, the accuracy of computation is verified by comparing the results with the experimental data of the prototype motor.

2. Analysis Model and Procedure

Fig. 1 shows the configuration of the original cooling fan SRM and its supply. This prototype motor has a wide dead zone and a low efficiency because it was designed in disregard of its supply state. The falling period of current is very short because of the switch-off voltage, which is over 5 times the switch-on voltage.

To resolve these problems, the supply converter was redesigned first to an asymmetric bridge converter. The supply is important to improve motor characteristics because a longer falling period of current can improve the torque ripple, but it can also raise a reverse torque. Therefore, the motor shapes are also changed in consideration of the converter. The motor variables are proposed as shown in Fig. 2. The redesign variables are stator pole arc, the ratio of stator pole arc, the existence of

* Dept. of Electrical Engineering, Changwon National University, Korea(jyecad@korea.com , motor@nc.namhae.ac.kr., jphong@sarim.changwon.ac.kr)

Received April 9, 2003; Accepted February 17, 2004

the dip and rotor slot depth as presented on the right side of Fig. 2. The ratio of stator pole arc is arc_1 versus arc_2. arc_1 is the longer side and the dip is on the other side, arc_2.

To improve the torque characters and efficiency, the variables are examined in 4 stages as follows:

1) Table 1 shows the initial combination of the variables. In this first stage, the switch turn-on angle is also considered because the switching angles influence current shape and magnetic characteristics of SRM. The base angle is 0°, the position in which the stator and rotor poles are unaligned, and minus means the reverse direction to rotation. The large characters 'S' and 'A' indicate symmetric and asymmetric pole shape, and the small characters 'a' and 'b' mean without and with dip, respectively. The numbers '10' and '20' are the absolute values of switch turn-on angle. Therefore, there are 8 types of models in the first stage.

2) In the second stage, the existence of the dip and stator pole arc is decided for 8 types of models selected in the first stage. The range of the stator pole arc is from 70° to 85° as shown in Table 2. According to the general design equations in [1] and [2], the minimum stator pole arc is 90° in the case of 4-stator pole and 2-rotor pole SRM, but that is difficult to fabricate.

3) The ratio of the stator pole arc is decided in the third stage. The ratio of the symmetric stator pole is 1:1, and the ratios of asymmetric stator poles are the others represented in Table II. The switch turn-on angle is still considered in this stage.

4) After the decision of stator pole shape and switch turn-on angle by stage 3, the rotor slot depth is selected in the last stage. The range of rotor slot depth is from 2 to 8mm as shown in Table 2.

Fig. 3 presents an analysis procedure by 2D FEM to select optimal pole shapes. For the first time, the linear inductance profiles are calculated at constant current conditions to find the exact unaligned position. And then, the magnetic performances of the models selected in each stage are calculated from the nonlinear dynamic analysis at constant voltage condition. This process helps to evaluate the different structure models and therefore, stator and rotor pole shapes can be decided for improvement of the motor efficiency and elimination of the dead zone.

Table 1 Classifications of Stator Pole Shapes

Switch Turn-on Angle (°)	Symmetric Pole ($arc_1 : arc_2 = 1 : 1$) without dip	with dip	Asymmetric Pole ($arc_1 : arc_2 = 5 : 4$) without dip	with dip
-10	S10a	S10b	A10a	A10b
-20	S20a	S20b	A20a	A20b

Table 2 Ranges of Variables

Stator Pole Arc (°)	70	75	80	85			
Ratio of Stator Pole Arc	1 : 1	9 : 8	5 : 4	3 : 2			
Rotor Slot Depth (mm)	2	3	4	5	6	7	8

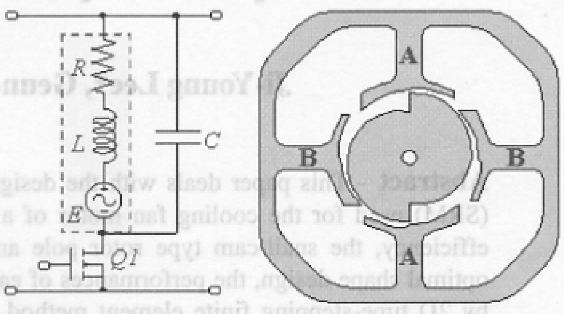

Fig. 1 Designed and fabricated drive and prototype motor

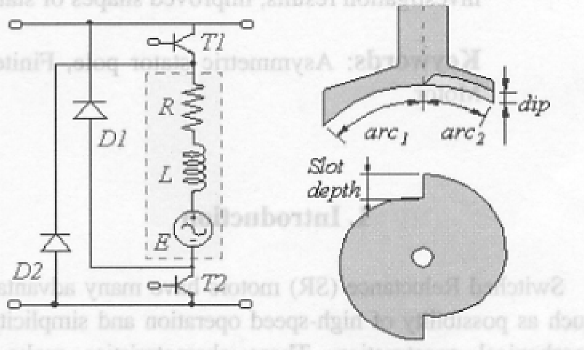

Fig. 2 Asymmetric bridge converter and detail configurations

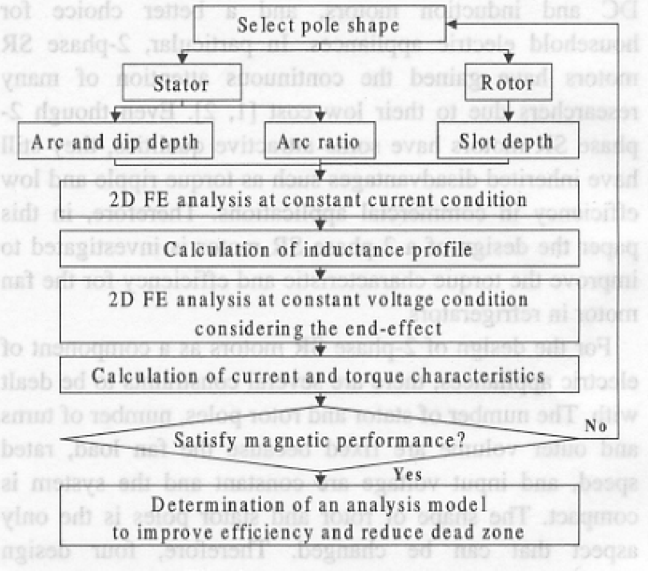

Fig. 3 Analysis procedure

3. Analysis Method

3.1 Electromagnetic Analysis

The electro-magnetic governing equation of SRM with field variable A is obtained by Maxwell's electromagnetic equation as follows:

$$\nabla \times (\frac{1}{\mu} \nabla \times A) = J_0 \quad (1)$$

where J_0 is the applied current density, A is the magnetic vector potential and μ is the magnetic permeability.

For the analysis of the dynamic characteristics, a voltage equation is coupled with equation (1) and then the system matrix is obtained by time difference schemes.

The method of the Maxwell stress tensor is used to calculate the static torque for the range of rotor position and phase excitation. Thus static torque is expressed according to the following equation (2).

$$T = \oint_s r \times P \, dS \quad (2)$$

where r is the distance vector of a point to axis rotation.

Equation (2) is obtained by the surface integration of a stress tensor vector P over an air gap enclosing the rotor surface S. The Maxwell stress tensor is given by (3) [3].

$$P = \frac{1}{\mu_0}(n \cdot B)B - \frac{1}{2\mu_0}B^2 n \quad (3)$$

where μ_0 is the permeability of free space, n is the normal vector to the surface S, and B is the magnetic flux density.

3.2 End Effect Calculation

From the electromagnetic analysis by 2D FEM, the linkage flux is calculated as the difference between vector potentials at both sides of excited coil in the stator pole. Then inductance is obtained by the ratio of the linkage flux and exciting current [4]. However, the 2D FEM is limited due to the inability to account for the axial fringing effect. For considering the 3D end effect, empirical formulations are developed from the analysis in [5]. Also, the equations in [6] and [7] are very useful. In this paper, the end effect for the unaligned and aligned inductance is calculated by the equation in [7].

4. Design and Analysis Result

4.1 Analysis and Measurement of Prototype

The comparison of measured and calculated inductance for the prototype motor is shown in Table 3. The error between the two inductances is under 5%. Fig. 4 shows the currents and torque of the machine. The current has been obtained through experimentation, the results of which are compared with those of the analysis by FEM. Since the aspects of the currents coincide, the torque can be expected as to be as shown in the lower part of Fig. 4. The efficiency of this motor is about 52.6%, but the dead zone is 16°.

4.2 Inductance Profiles

Fig. 5 presents the linear inductances of each analysis model, which consists of the variables in Tables 1 and 2. In this figure, the rotor positions are not absolute, and the start point (0°) is where the inductance is minimal. The profiles are different from each other with respect to stator pole arc and the existence of dip, but they are identical for the symmetric and asymmetric pole shapes because saturation is neglected in the magnetic materials. A wider pole arc creates a longer increase span and the dip creates a sharp drop in the decrease span.

4.3 Stator and Rotor Pole Design

Fig. 6 shows the comparison of the effective minimum torque (EMT) and the efficiency of the models in Table 1 with respect to the stator pole arc in Table 2. The EMT is the ratio of minimum torque to average torque. When this value is greater than zero, there is no dead zone, and the relative magnitude allows comparison of torque ripple of each model. In most cases, the existence of dip and smaller stator pole arc creates higher EMT and lower efficiency.

Fig. 7 shows the results of analysis for the ratio of stator pole arc when the stator pole arc is 80° without dip. The EMT and the efficiency depend on the ratio of the stator pole and the switch turn-on angle. The highest efficiency is obtained when the ratio is 5:4 and switch turn-on angle is –10°. The EMT of this pole shape is also greater than zero.

After the decision of stator pole shape and switch turn-on angle, the rotor slot depth is selected for the last stage. Fig. 8 shows the average torque, the EMT and the efficiency with rotor slot depth. All performances increase until the rotor slot depth is 6mm.

From the above investigation, the SRM for the cooling fan is redesigned. The configuration and the performances are numerically compared with the prototype in Table 4. Efficiency is increased by 2.1% and the dead zone is eliminated. The torque profile of redesigned motors is presented in Fig. 9 and this is graphically compared with Fig. 4.

5. Conclusions

This paper demonstrates the effect of stator and rotor pole shapes on torque characteristics for 2-phase SRM. The detail trends of the performance according to various design parameters are investigated by 2D time stepping FEM coupled with voltage equation. As the redesigned results indicate, the improved motor has an asymmetric stator pole and a snail-cam rotor with deeper slot depth. The efficiency of the redesigned motor is higher than that of the original prototype and the dead zone is completely eliminated.

Table 3 Comparison of Measured and Calculated Inductances

	Measured Inductance (mH)	Calculated Inductance (mH) 2D FEM	End Effect	Sum	Error (%)
Aligned	173.18	169.07	12.41	181.48	4.79
Unaligned	79.78	50.86	27.01	77.87	2.39

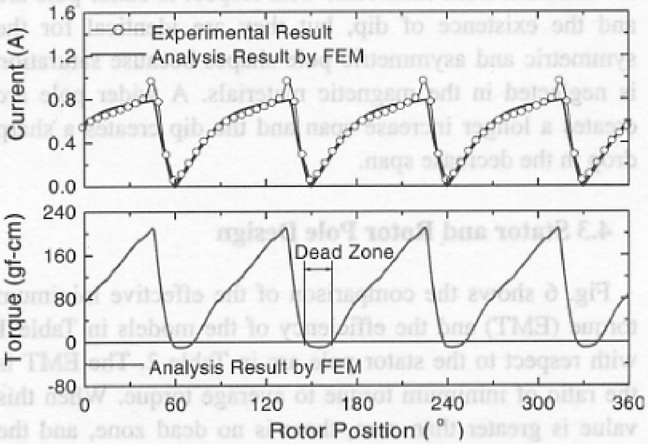

Fig. 4 Current (upper) and torque (lower) of prototype

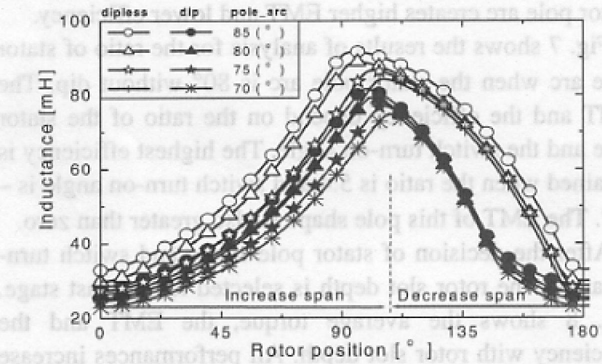

Fig. 5 Inductance profiles of symmetric stator pole without dip, and symmetric stator pole with dip for rotor position and stator pole arc

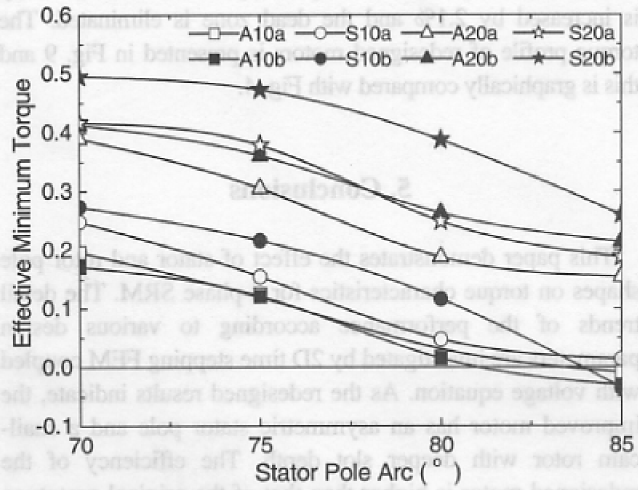

(a)

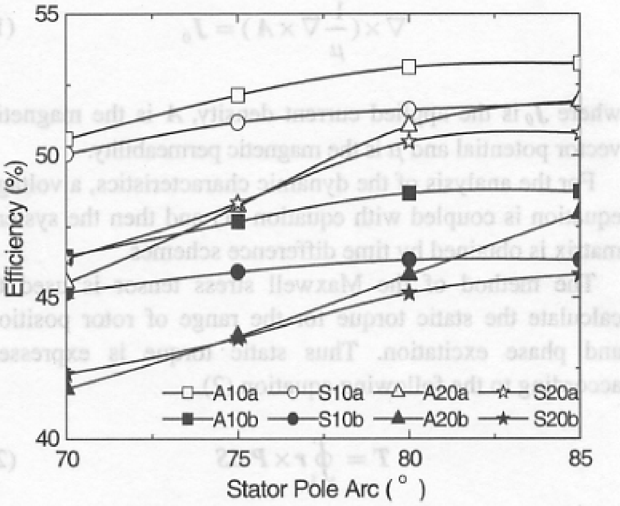

(b)

Fig. 6 Effective minimum torque (a) and efficiency (b) with respect to stator pole arc

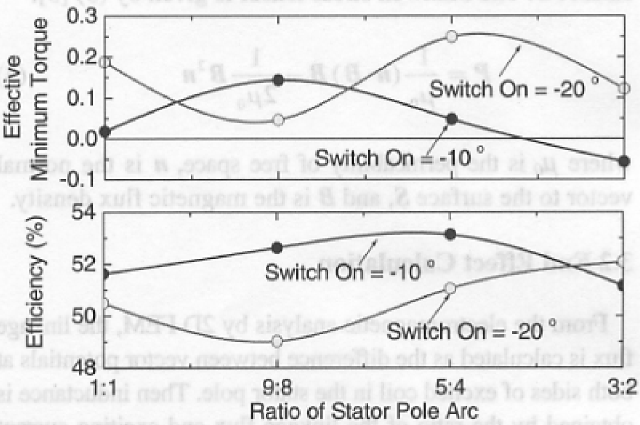

Fig. 7 Effective minimum torque (upper) and efficiency (lower) with respect to the ratio of stator pole arc

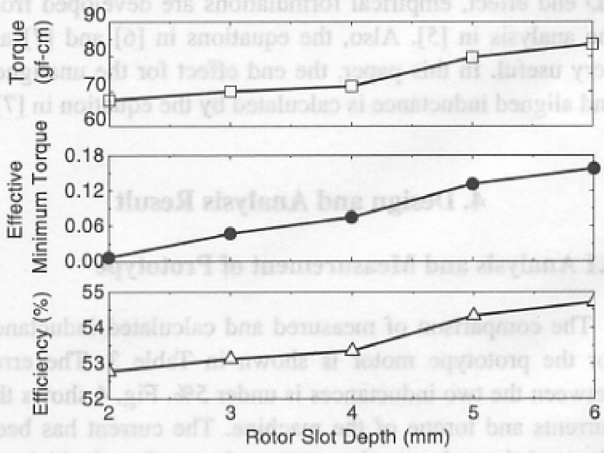

Fig. 8 Average torque (upper), effective minimum torque (middle) and efficiency (lower) with respect to the rotor slot depth

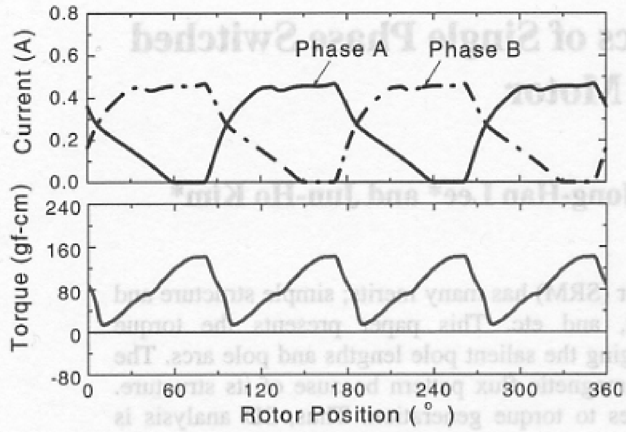

Fig. 9 Current (upper) and torque (lower) of improved model

Table 4 Comparison of Prototype and Improved Model

	Prototype	Improved Model
Stator Pole Arc (°)	85	80
Ratio of Stator Pole Arc	9 : 8	5 : 4
Existence of Dip	Yes	No
Rotor Slot Depth (mm)	4	6
Average Torque (kgf-cm)	79.6	83.0
Efficiency (%)	52.6	54.7
Dead Zone (°)	16	0

References

[1] J. E. Miller, *Switched Reluctance Motors and Their Control*, Magna physics publishing and Clarendon Press Oxford, 1993.

[2] P. J. Lawrenson and el. "Variable-speed switched reluctance motors," *IEE Proceeding*, vol. 127, pp. 253-265, July, 1980

[3] M. J. DeBortoli and S. J. Salon, "Computation of forces and torque in electromagnetic devices using the finite element method," *International Conference on Electrical Machines*, pp. 699-705, August, 1990

[4] Koichi Koibuchi and el, "A Basic Study for Optimal Design of Switched Reluctance Motor by Finite Element Method," *IEEE Trans. on Magnetics*, vol. 33, pp. 2077-2080, March, 1997

[5] J. Corda and J. M. Stephenson, "Analytical estimation of the minimum and maximum inductances of a double-salient motor," *in Proceedings of the International Conference on Stepping Motors and Systems*, Lees, U. K., pp.50-59, September, 1979

[6] Yifan Tang, "Characterization, Numerical Analysis, and Design of Switched Reluctance Motors," *IEEE Trans. on Industry Application*, vol. 33, pp. 1544-1552, November/December, 1997.

[7] *User's Manual of PC-SRD VERSION 7.0*, SPEED CONSORTIUM, 1999

Ji-Young Lee

She received her B.S. and M.S. degrees in Electrical Engineering from Changwon National University. She is presently pursuing a Ph.D. at the same University. Her research interests are in the area of design and analysis of reluctance motors.

Tel: 82-55-262-5966

Geun-Ho Lee

He received his B.S. and M.S. degrees in Electrical Engineering from Hanyang University. He is presently pursuing a Ph.D. at Changwon National University. He is a Fulltime Lecturer at Gyeongnam Provincial Namhae College. His research interest is in the area of electrical motor control.

Tel: 82-55-860-5354

Jung-Pyo Hong

He received his B.S., M.S. and Ph.D. degrees in Electrical Engineering from Hanyang University. He is presently an Associate Professor at Changwon National University. His research interests are in the area of design and analysis of electric machines.

Tel: 82-55-279-7510